

## Supramolecular Chemistry

International Edition: DOI: 10.1002/anie.201800490  
German Edition: DOI: 10.1002/ange.201800490Hierarchical Assembly of an Interlocked  $M_8L_{16}$  Container

Witold M. Bloch,\* Julian J. Holstein, Birger Dittrich, Wolf Hiller, and Guido H. Clever\*

**Abstract:** The self-assembly of eight  $Pd^{II}$  cations and sixteen phenanthrene-derived bridging ligands with  $60^\circ$  bite angles yielded a novel  $M_8L_{16}$  metallocupramolecular architecture composed of two interlocked  $D_{4h}$ -symmetric barrel-shaped containers. Mass spectrometry, NMR spectroscopy, and X-ray analysis revealed this self-assembled structure to be a very large “Hopf link” catenane featuring channel-like cavities, which are occupied by  $NO_3^-$  anions. The importance of the anions as catenation templates became imminent when we observed the nitrate-triggered structural rearrangement of a mixture of  $M_3L_6$  and  $M_4L_8$  assemblies formed in the presence of  $BF_4^-$  anions into the same interlocked molecule. Furthermore, the densely packed structure of the  $M_8L_{16}$  catenane was exploited in the preparation of a hexyloxy-functionalized analogue, which further self-assembled into vesicle-like aggregates in a reversible manner.

Mechanically interlocked structures continue to spark scientific interest and curiosity owing to their aesthetic appeal and the dynamic properties that are introduced by the mechanical bond.<sup>[1]</sup> Although their preparation initially posed a synthetic challenge, the utilization of molecular templates<sup>[2]</sup> and the implementation of reversible covalent bonds<sup>[3]</sup> have resulted in high-yielding and facile syntheses. In this regard, the highly directional coordinative bond has been the basis of a variety of interpenetrated structures, such as catenanes,<sup>[4]</sup> rotaxanes,<sup>[5]</sup> knots,<sup>[6]</sup> Borromean rings,<sup>[7]</sup> and more.<sup>[8]</sup>

Among the plethora of possible metal and ligand combinations,  $Pd^{II}$  cations together with N-donor bridging ligands

represent a robust and reliable combination widely utilized in the formation of hollow and interlocked metallocupramolecular structures.<sup>[8b,9]</sup> For assemblies obeying  $Pd_nL_{2n}$  stoichiometry ( $n=6, 12, 24, 30\dots$ ), Fujita and co-workers have demonstrated the topological dependence of the structure of hollow polyhedra on obtuse ligand bite angles.<sup>[10]</sup> This work was recently expanded to the synthesis of a giant  $Pd_{48}L_{96}$  Goldberg polyhedron.<sup>[10e]</sup> More acute ligand bite angles ( $\geq 60^\circ$ ) often yield  $Pd_3L_6$  and  $Pd_4L_8$  barrel-shaped containers or  $Pd_4L_8$  doubly bridged tetrahedra (Figure 1),<sup>[11]</sup> whilst

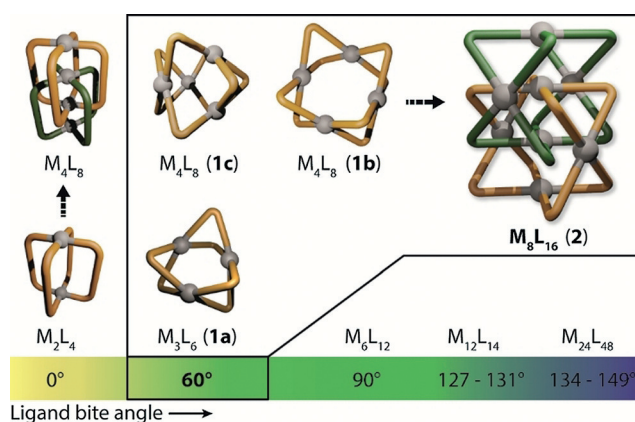


**Figure 1.** Comparison of the known  $M_nL_{2n}$  ( $M = Pt^{II}$  or  $Pd^{II}$ ) structures according to the bite angle of their constituent ligands with the catenated  $M_8L_{16}$  architecture **2**. Metal-mediated self-assembly of a ligand with a  $60^\circ$  bite angle can give rise to  $M_3L_6$  (**1a**) or  $M_4L_8$  structures (**1b** or **1c**). In previous studies, only  $M_2L_4$  cage structures were shown to undergo catenation to give  $M_4L_8$  interlocked dimers.

ligands with a parallel orientation of donors form lantern-shaped  $Pd_2L_4$  coordination cages.<sup>[9]</sup> Catenation of the latter cages results in a larger family of  $Pd_4L_8$  dimeric structures with a partitioned cavity capable of allosterically binding charged<sup>[12]</sup> and neutral<sup>[13]</sup> guest molecules. Under certain circumstances, these types of ligands also form a triply catenated link.<sup>[14]</sup> More recently, the close proximity of electron donor/acceptor moieties in mixed-ligand  $Pd_4L_8$  interpenetrated cages has been exploited to study charge-transfer phenomena,<sup>[15]</sup> demonstrating that interlocked structures can also serve as platforms to examine interactions of densely packed functionalities.

Despite the vast structural diversity of reported  $Pd_nL_{2n}$  polyhedral structures, interpenetrated assemblies larger than the  $Pd_4L_8$  dimeric cages remained hitherto undiscovered. Herein, we report the assembly of an interlocked metallocupramolecule with the formula  $M_8L_{16}$  ( $M = Pd^{II}$ ), which is the largest  $Pd_nL_{2n}$  catenane reported to date. Palladium-mediated self-assembly of the dimeric structure was achieved

[\*] Dr. W. M. Bloch, Dr. J. J. Holstein, Prof. Dr. W. Hiller, Prof. Dr. G. H. Clever

Department of Chemistry and Chemical Biology  
TU Dortmund University  
Otto-Hahn-Straße 6, 44227 Dortmund (Germany)  
E-mail: guido.clever@tu-dortmund.de

Dr. W. M. Bloch  
Department of Chemistry and Centre for Advanced Nanomaterials  
School of Physical Sciences  
The University of Adelaide, Adelaide (Australia)  
E-mail: witold.bloch@adelaide.edu.au

Priv.-Doz. Dr. B. Dittrich  
Institute for Inorganic Chemistry and Structural Chemistry  
Heinrich-Heine University Düsseldorf  
Universitätsstraße 1, 40225 Düsseldorf (Germany)

Supporting information and the ORCID identification number(s) for the author(s) of this article can be found under:  
<https://doi.org/10.1002/anie.201800490>.

© 2018 The Authors. Published by Wiley-VCH Verlag GmbH & Co. KGaA. This is an open access article under the terms of the Creative Commons Attribution Non-Commercial License, which permits use, distribution and reproduction in any medium, provided the original work is properly cited, and is not used for commercial purposes.

with  $\text{Pd}(\text{NO}_3)_2$  and a rigid bis(monodentate) ligand **L** with a bite angle of  $60^\circ$ . The presence of  $\text{NO}_3^-$  anions is crucial for the formation of the large catenane, and can also trigger the structural rearrangement of a mixture of  $\text{Pd}_3\text{L}_6$  and  $\text{Pd}_4\text{L}_8$  assemblies formed in the presence of  $\text{BF}_4^-$  anions into the same interpenetrated structure. Through alkyl functionalization of the ligand backbone, an amphiphilic catenane was prepared that further self-assembled into vesicle-like aggregates, demonstrating that the densely packed nature of the  $\text{Pd}_8\text{L}_{16}$  architecture can be utilized as a platform for higher-order supramolecular aggregation.

Phenanthrene-based ligand **L**<sup>1</sup> (Figure 2) readily underwent self-assembly with  $[\text{Pd}(\text{CH}_3\text{CN})_4](\text{BF}_4)_2$  to form a  $D_{4h}$ -symmetric  $\text{Pd}_4\text{L}_8$  (**1b**) container in DMSO as the only product.<sup>[11c]</sup> In  $\text{CD}_3\text{CN}$ , however, a 1:2:0.2 mixture of a  $D_{3h}$ -symmetric  $\text{Pd}_3\text{L}_6$  (**1a**) container, **1b**, and a  $D_{2d}$ -symmetric

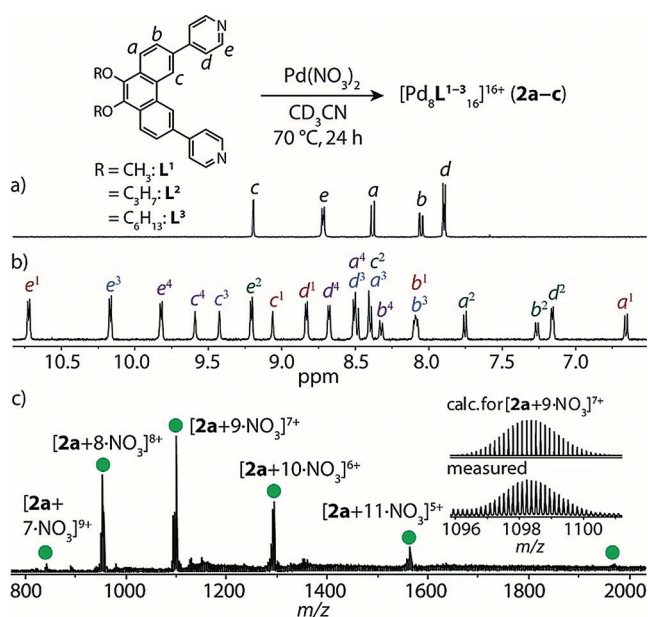


**Figure 2.** Top: Reaction equation representing the formation of  $\text{Pd}_8\text{L}_{16}$  (**2a–2c**). Bottom:  $^1\text{H}$  NMR spectra (500 MHz,  $\text{CD}_3\text{CN}$ ,  $25^\circ\text{C}$ ) of a) ligand **L**<sup>1</sup> and b) **2a**. c) ESI-MS spectrum of **2a** with the measured and calculated isotope patterns of  $[\mathbf{2a}+9\text{NO}_3]^{7+}$  shown in the inset.

tetrahedron (**1c**) was obtained (Figure 1).<sup>[16]</sup> As both solvent and anion are known to dramatically affect the assembly of coordination cage structures,<sup>[9d,11]</sup> we carried out further investigations, including the reaction of **L**<sup>1</sup> with  $\text{Pd}(\text{NO}_3)_2$ . Self-assembly in the presence of nitrate anions again yielded **1b** as the major product in DMSO (Figure S10); however, in  $\text{CD}_3\text{CN}$ , we observed an entirely different outcome.

Heating a 2:1 mixture of **L**<sup>1</sup> and  $\text{Pd}(\text{NO}_3)_2$  in  $\text{CD}_3\text{CN}$  at  $70^\circ\text{C}$  for 24 h resulted in the quantitative formation of a new species (**2a**), as indicated by  $^1\text{H}$  NMR spectroscopy and ESI mass spectrometry. In the  $^1\text{H}$  NMR spectrum, a total of 20 aromatic signals were identified in the range of  $\delta = 6.6$ – $10.7$  ppm (compared with 5 aromatic signals for **L**<sup>1</sup>), along with four signals in the region of the methoxy protons (Figures 2 and S11). ESI-MS analysis gave a spectrum with several prominent peaks consistent with the formula

$[\text{Pd}_8\text{L}_{16}+n\text{NO}_3]^{(16-n)+}$  ( $n=7$ – $12$ ; Figure 2c). By COSY NMR analysis, we identified four distinct sets of aromatic signals of equal ratios for **L**<sup>1</sup>. Further analysis by  $^1\text{H}$ - $^1\text{H}$  NOESY revealed numerous cross-peaks (Figure S14), including notable through-space contacts between the  $\text{H}_c$  protons of sets 1/2 and 3/4. We therefore postulated that the fourfold splitting is due to **L**<sup>1</sup> being in two different chemical environments and losing its twofold symmetry in **2a**. The exclusive formation of **2a** was further confirmed by DOSY NMR analysis (Figure S16), which revealed that all of the assigned proton signals correspond to the same diffusion coefficient, with the derived hydrodynamic radius (1.24 nm) pointing towards a rather compact structure.

According to the empirical predictions for  $\text{Pd}_n\text{L}_{2n}$  assemblies,<sup>[10]</sup> a structure with a composition of  $\text{Pd}_8\text{L}_{16}$  is incompatible with a spherical, hollow topology, unless it is a transient intermediate towards larger  $\text{Pd}_{12}\text{L}_{24}$  polyhedra.<sup>[10d]</sup> In light of the fourfold signal splitting observed in the  $^1\text{H}$  NMR spectrum of **2a**, our  $\text{Pd}_8\text{L}_{16}$  assembly is therefore likely to be composed of two interpenetrating  $\text{Pd}_4\text{L}_8$  subunits. To gain insight into whether the possible monomeric  $\text{Pd}_4\text{L}_8$  assemblies (**1b** or **1c**) are transient intermediates preceding **2a**, time-resolved  $^1\text{H}$  NMR experiments were performed on a 2:1 mixture of **L**<sup>1</sup> and  $\text{Pd}(\text{NO}_3)_2$  at  $70^\circ\text{C}$  in MeCN (Figure S17). Only the proton resonances of **2a** evolved gradually over 20 h, and no other species were detected, suggesting that any intermediates involved in the self-assembly process are polymeric or short-lived in solution.

Owing to difficulties encountered with obtaining crystals of **2a** that are suitable for X-ray analysis, we focused on modifying the solubility of the catenane by utilizing a pro-poxy-functionalized ligand **L**<sup>2</sup>. Under the same reaction conditions as for **2a**, the reaction of **L**<sup>2</sup> with  $\text{Pd}(\text{NO}_3)_2$  gave an analogous  $\text{Pd}_8\text{L}_{16}$  interlocked structure (**2b**), as confirmed by  $^1\text{H}$  NMR spectroscopy and ESI-MS analysis (Figures S18–S21). Single crystals (diffracting up to  $1.28 \text{ \AA}$  with synchrotron radiation)<sup>[17]</sup> were grown by slow vapor diffusion of diisopropyl ether into a concentrated  $\text{CD}_3\text{CN}$  solution of **2b**, enabling unambiguous structure elucidation by X-ray crystallography. **2b** crystallized in the monoclinic space group  $P2_1/n$ , with one  $\text{Pd}_8\text{L}_{16}$  molecule in the asymmetric unit. The large interpenetrated structure, which is composed of two interlocked  $D_{4h}$ -symmetric containers,<sup>[18]</sup> can be described as a “Hopf link” (Figure 3) with  $D_{2d}$  symmetry.

In the structure of **2b**, the  $\text{Pd}_4\text{L}_8$  monomers are geometrically related to one another by a  $90^\circ$  rotation along the major  $C_2$  axis, creating an even partition of three channel-like cavities, each accommodating a  $\text{NO}_3^-$  counterion (Figure 3a). The central cavity is enclosed by phenanthrene moieties of **L**<sup>2</sup>, which participate in offset  $\pi$ -stacking with an average separation of  $3.7 \text{ \AA}$ . In contrast to the  $\text{Pd}_4\text{L}_8$  interpenetrated cages,<sup>[8b]</sup> **2b** appears to be sterically restricted from mechanical movement owing to the respective tilt of the ligands between adjacent  $\text{Pd}_4\text{L}_8$  units. In addition to the three  $\text{NO}_3^-$  anions found along the  $C_2$  axis, four more (of a total of 13 located in the Fourier difference map) were found within the interpenetrated structure; however, not all of them occupied defined cavities. For example, **2b** contains four smaller cavities located perpendicular to the major  $C_2$  axis along the



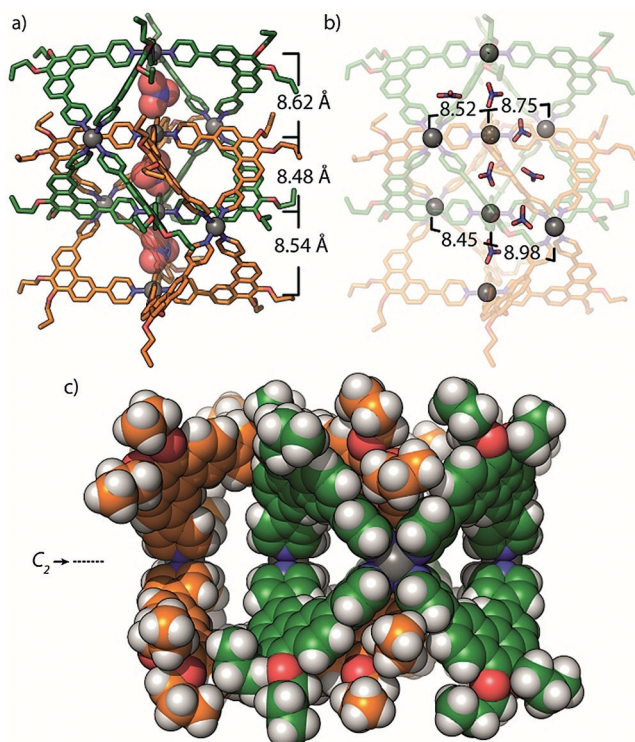


**Figure 3.** X-ray structure of **2b**:<sup>[24]</sup> a) Showing Pd...Pd distances and encapsulated  $\text{NO}_3^-$  anions along the major  $C_2$  axis, b) highlighting the Pd...Pd distances of cations orthogonal to the major  $C_2$  axis, c) a space-filling representation of the [2]catenane with  $\text{NO}_3^-$  anions removed for clarity.

$\text{Pd}_3$  planes (Figure 3b), with only two of the four cavities being occupied. Accordingly, the Pd...Pd separations for the empty cavities are 0.2–0.5 Å shorter than those of the filled cavities.<sup>[19]</sup>

Next, we examined whether  $\text{NO}_3^-$  anions trigger a transformative rearrangement of the mixture of **1a**, **1b**, and **1c** that is formed when  $L^1$  is reacted with  $[\text{Pd}(\text{CH}_3\text{CN})_4](\text{BF}_4)_2$ <sup>[16]</sup> in  $\text{CD}_3\text{CN}$  (during the course of our studies, a single crystal of **1c** was isolated and analyzed by X-ray crystallography, further supporting **1c** as one of the Pd-mediated assemblies of  $L^1$ ; Figures 4b and S38–S40). The mixture of **1a**, **1b**, and **1c** was

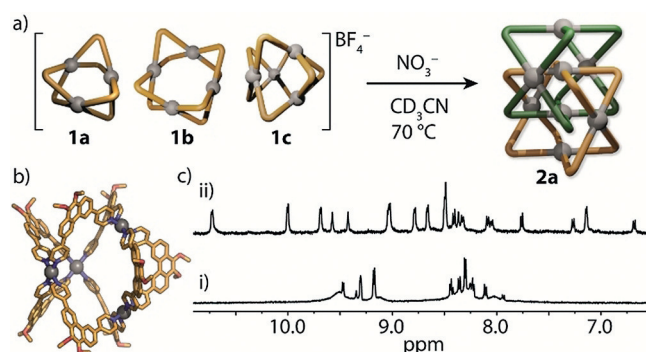


**Figure 4.** a) The  $\text{NO}_3^-$ -mediated transformation of **1a–1c** into **2a**. b) X-ray structure of **1c**.<sup>[24]</sup> c)  $^1\text{H}$  NMR spectra (500 MHz,  $\text{CD}_3\text{CN}$ ) of i) **1a–1c** and ii) the same mixture after heating for 24 h in the presence of  $\text{NO}_3^-$  anions.

therefore heated at 70 °C for 24 h with 4, 8, and 12 equivalents of  $\text{NO}_3^-$ . In each case,  $^1\text{H}$  NMR spectroscopy revealed that **2a** was formed exclusively (Figure 4); however, the reaction proceeded with the highest yield when 8 equivalents of  $\text{NO}_3^-$  were used (Figure S27). ESI-MS of this sample confirmed the structural conversion of **1a–1c** into **2a** as it revealed signals corresponding to  $[\text{Pd}_8L_{16} + nX]^{(16-n)+}$  ( $n=8–11$ ,  $X=\text{Cl}^-$ ,  $\text{NO}_3^-$ , and  $\text{BF}_4^-$ ), with each signal distribution comprising a bias towards  $X=8\text{NO}_3^-$  and  $(8-n)\text{BF}_4^-$  (Figure S28). To gain further insight into the role of the nitrate anions in the system, we performed the same transformation with a  $^{15}\text{N}$ -labeled  $\text{NO}_3^-$  source. Inverse-gated  $^{15}\text{N}$  NMR analysis revealed a single  $^{15}\text{N}$  signal, which corresponds to the free  $^{15}\text{NO}_3^-$  signal of the tetrabutylammonium salt used in the transformation (Figure S29). This indicates that the  $\text{NO}_3^-$  anions are not tightly bound and are free to exchange with free  $\text{NO}_3^-$  in the solvent, which is consistent with the channel-like cavities observed in the X-ray structure of **2b**. The reason for why catenation is observed only in the presence of  $\text{NO}_3^-$  anions could therefore be related to their optimal size as templates for this dimer.<sup>[12b,14,20]</sup> Indeed, **1a–1c** were not transformed into the catenated product upon extended heating (70 °C, 24 h) or in the presence of  $\text{PF}_6^-$  anions (Figures S9 and S31).

Finally, we examined whether the structurally dense nature of the  $\text{Pd}_8L_{16}$  [2]catenane can be utilized as a platform for further functionalization and supramolecular aggregation. It is worth noting that hierarchical aggregates of nanocages have scarcely been reported, and the underlying mechanisms of such systems primarily rely upon counterion-mediated interactions and  $\pi$ -stacking.<sup>[21]</sup> To promote a different aggregation pathway, we prepared a dihexyloxy-functionalized ligand ( $L^3$ ) for the palladium-mediated self-assembly of amphiphilic catenane **2c** (Figures S22–S26). Remarkably, in MeCN, **2c** rapidly and spontaneously further self-assembled into a colloid of nanoscale vesicular aggregates by virtue of the dense hydrophobic interactions between molecules of **2c** (Figure 5). This is in contrast to the behavior of **2a** and **2b**,

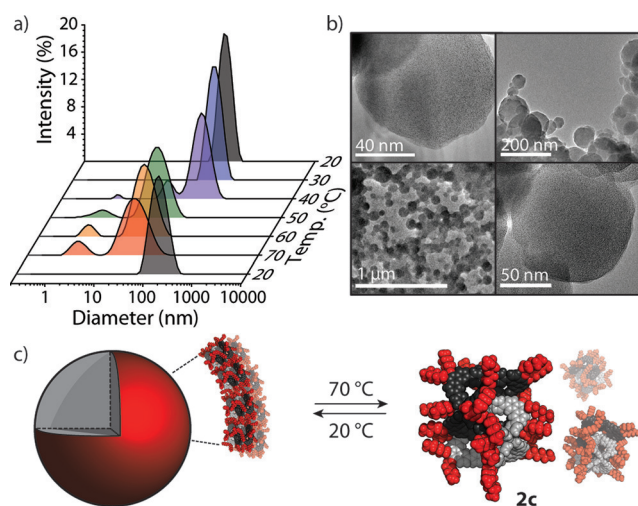


**Figure 5.** a) Variable-temperature DLS. b) TEM images of **2c**. c) Temperature-dependent aggregation of **2c** (plausible model based on the X-ray structure of **2b**).

which remain in solution owing to the shorter alkyl chains of their respective ligands. At 25 °C, a <sup>1</sup>H NMR spectrum of a cloudy solution of **2c** revealed the complete absence of proton resonances. At elevated temperatures (50–70 °C), however, the solution of **2c** became completely transparent, and the characteristic NMR spectroscopic signature of the interlocked molecule was observed (Figures S22 and S23). Dynamic light scattering (DLS) analysis of **2c** revealed particles with diameters of 150 ± 45 nm (PDI = 0.09) at 20 °C, which were observed to incrementally swell upon dilution (Figure S32), which is indicative of a vesicular-type assembly.<sup>[22]</sup> Variable temperature (VT) DLS revealed that this aggregate begins to disassemble between 40 and 50 °C, at which point a smaller aggregate (36.2 ± 20.4 nm) is formed along with particles measuring 2.3 ± 0.7 nm in diameter, the latter coinciding with the approximate dimensions of a single molecule of **2c**. Interestingly, cooling the sample back to 20 °C resulted in the recovery of the original, approximately 150 nm large aggregate (Figure 5a), with the MeCN solution becoming cloudy once again. The reversibility of the temperature-dependent supramolecular aggregation was demonstrated over three cycles by DLS with no detectable degradation (Figure S33). High-resolution TEM analysis of **2c** (Figures 5b and S34) confirmed the presence of spherical particles, albeit with a slightly broader distribution (80–200 nm).<sup>[23]</sup> This is in contrast to the TEM analysis of **2a**, which revealed small particles with diameters of approximately 3 nm, which correspond to non-aggregated molecules of **2a** (Figure S36). This observation further supports our hypothesis that the hydrophobic hexyloxy chains in **2c** promote hierarchical aggregation, which is facilitated by the structurally dense nature of this type of interlocked architecture.

In conclusion, we have reported the self-assembly of a 24-component Pd<sub>8</sub>L<sub>16</sub> [2]catenane composed of two interlocked D<sub>4h</sub>-symmetric Pd<sub>4</sub>L<sub>8</sub> barrel-shaped containers. The formation of the large catenane was shown to depend on the presence of NO<sub>3</sub><sup>-</sup> counterions by NMR, ESI-MS, and crystallographic analysis. We also showed that NO<sub>3</sub><sup>-</sup> anions can trigger the structural rearrangement of a mixture of Pd<sub>3</sub>L<sub>6</sub> and Pd<sub>4</sub>L<sub>8</sub> assemblies into the same interpenetrated product. Indeed, the X-ray crystal structure of **2b** revealed that the channel-like cavities are occupied by NO<sub>3</sub><sup>-</sup> anions, which not only charge-balance the structure but also facilitate the interpenetration of the Pd<sub>4</sub>L<sub>8</sub> barrel-shaped monomers. Exohedral functionalization of the structurally dense catenane with hexyloxy chains resulted in the hierarchical assembly of vesicle-like aggregates, which could be reversibly assembled and disassembled by a change in temperature. We are currently investigating the use of this aggregate as a molecular delivery and release vessel.

## Acknowledgements

We thank Dr. Andreas Brockmeyer and Dr. Petra Janning (Max-Planck Institute for Molecular Physiology, Dortmund) and Dr. Holm Frauendorf (Georg-August University Göttingen) for mass spectrometry, Dr. Ashley Slattery (Adelaide Microscopy) for assistance with TEM measurements, and

Björn Holzapfel (TU Dortmund) for assistance with DLS measurements. W.M.B. thanks the Alexander von Humboldt Foundation for a postdoctoral fellowship and acknowledges support through an Adelaide University Ramsay Fellowship. This work has been financially supported by an ERC Consolidator grant 683083 (RAMSES) and the DFG-funded Cluster of Excellence RESOLV (EXC 1069). The crystallographic experiments for **1c** were performed at the PXII (X06SA) beamline of the Swiss Light Source, Paul Scherrer Institut, Villigen, Switzerland. Diffraction data for **2b** were collected at PETRA III at DESY, a member of the Helmholtz Association (HGF). We thank Saravanan Panneerselvam for assistance in using synchrotron beamline P11 (I-20170404).<sup>[17]</sup>

## Conflict of interest

The authors declare no conflict of interest.

**Keywords:** catenanes · interlocked structures · self-assembly · structural transformations · supramolecular chemistry

**How to cite:** *Angew. Chem. Int. Ed.* **2018**, *57*, 5534–5538  
*Angew. Chem.* **2018**, *130*, 5632–5637

- [1] a) J. F. Stoddart, *Chem. Soc. Rev.* **2009**, *38*, 1802–1820; b) M. S. Vickers, P. D. Beer, *Chem. Soc. Rev.* **2007**, *36*, 211–225; c) M. Janke, Y. Rudzevich, O. Molokanova, T. Metzroth, I. Mey, G. Diezemann, P. E. Marszalek, J. Gauss, V. Bohmer, A. Janshoff, *Nat. Nanotechnol.* **2009**, *4*, 225–229; d) J.-P. Collin, C. Dietrich-Buchecker, P. Gaviña, M. C. Jimenez-Molero, J.-P. Sauvage, *Acc. Chem. Res.* **2001**, *34*, 477–487; e) *Angew. Chem. Int. Ed.* **2016**, *55*, 13925; *Angew. Chem.* **2016**, *128*, 14129.
- [2] a) C. D. Meyer, C. S. Joiner, J. F. Stoddart, *Chem. Soc. Rev.* **2007**, *36*, 1705–1723; b) K. M. Mullen, P. D. Beer, *Chem. Soc. Rev.* **2009**, *38*, 1701–1713; c) J.-F. Ayme, J. E. Beves, C. J. Campbell, D. A. Leigh, *Chem. Soc. Rev.* **2013**, *42*, 1700–1712; d) M. Denis, S. M. Goldup, *Nat. Rev. Chem.* **2017**, *1*, 61.
- [3] a) G. Zhang, O. Presly, F. White, I. M. Oppel, M. Mastalerz, *Angew. Chem. Int. Ed.* **2014**, *53*, 5126–5130; *Angew. Chem.* **2014**, *126*, 5226–5230; b) T. Hasell, X. Wu, J. T. Jones, J. Bacsá, A. Steiner, T. Mitra, A. Trewin, D. J. Adams, A. I. Cooper, *Nat. Chem.* **2010**, *2*, 750–755.
- [4] a) M. Fujita, *Acc. Chem. Res.* **1999**, *32*, 53–61; b) S. Prusty, S. Krishnaswamy, S. Bandi, B. Chandrika, J. Luo, J. S. McIndoe, G. S. Hanan, D. K. Chand, *Chem. Eur. J.* **2015**, *21*, 15174–15187; c) C. S. Wood, T. K. Ronson, A. M. Belenguer, J. J. Holstein, J. R. Nitschke, *Nat. Chem.* **2015**, *7*, 354–358.
- [5] a) J.-P. Sauvage, *Acc. Chem. Res.* **1998**, *31*, 611–619; b) J. E. Beves, B. A. Blight, C. J. Campbell, D. A. Leigh, R. T. McBurney, *Angew. Chem. Int. Ed.* **2011**, *50*, 9260–9327; *Angew. Chem.* **2011**, *123*, 9428–9499.
- [6] a) D. M. Engelhard, S. Freye, K. Grohe, M. John, G. H. Clever, *Angew. Chem. Int. Ed.* **2012**, *51*, 4747–4750; *Angew. Chem.* **2012**, *124*, 4828–4832; b) J. Guo, P. C. Mayers, G. A. Breault, C. A. Hunter, *Nat. Chem.* **2010**, *2*, 218–222; c) P. E. Barran, H. L. Cole, S. M. Goldup, D. A. Leigh, P. R. McGonigal, M. D. Symes, J. Wu, M. Zengerle, *Angew. Chem. Int. Ed.* **2011**, *50*, 12280–12284; *Angew. Chem.* **2011**, *123*, 12488–12492.
- [7] a) S.-L. Huang, Y.-J. Lin, Z.-H. Li, G.-X. Jin, *Angew. Chem. Int. Ed.* **2014**, *53*, 11218–11222; *Angew. Chem.* **2014**, *126*, 11400–11404; b) K. S. Chichak, S. J. Cantrill, A. R. Pease, S.-H. Chiu,

- G. W. V. Cave, J. L. Atwood, J. F. Stoddart, *Science* **2004**, *304*, 1308–1312.
- [8] a) S. D. P. Fielden, D. A. Leigh, S. L. Woltering, *Angew. Chem. Int. Ed.* **2017**, *56*, 11166–11194; *Angew. Chem.* **2017**, *129*, 11318–11347; b) M. Frank, M. D. Johnstone, G. H. Clever, *Chem. Eur. J.* **2016**, *22*, 14104–14125; c) K. E. Horner, M. A. Miller, J. W. Steed, P. M. Sutcliffe, *Chem. Soc. Rev.* **2016**, *45*, 6432–6448; d) J. E. M. Lewis, P. D. Beer, S. J. Loeb, S. M. Goldup, *Chem. Soc. Rev.* **2017**, *46*, 2577–2591; e) R. S. Forgan, J.-P. Sauvage, J. F. Stoddart, *Chem. Rev.* **2011**, *111*, 5434–5464; f) S.-L. Huang, T. S. A. Hor, G.-X. Jin, *Coord. Chem. Rev.* **2017**, *333*, 1–26.
- [9] a) G. H. Clever, P. Punt, *Acc. Chem. Res.* **2017**, *50*, 2233–2243; b) M. Han, D. M. Engelhard, G. H. Clever, *Chem. Soc. Rev.* **2014**, *43*, 1848–1860; c) W. M. Bloch, G. H. Clever, *Chem. Commun.* **2017**, *53*, 8506–8516; d) R. Chakrabarty, P. S. Mukherjee, P. J. Stang, *Chem. Rev.* **2011**, *111*, 6810–6918.
- [10] a) Q.-F. Sun, J. Iwasa, D. Ogawa, Y. Ishido, S. Sato, T. Ozeki, Y. Sei, K. Yamaguchi, M. Fujita, *Science* **2010**, *328*, 1144–1147; b) J. Bunzen, J. Iwasa, P. Bonakdarzadeh, E. Numata, K. Rissanen, S. Sato, M. Fujita, *Angew. Chem. Int. Ed.* **2012**, *51*, 3161–3163; *Angew. Chem.* **2012**, *124*, 3215–3217; c) H. Yokoyama, Y. Ueda, D. Fujita, S. Sato, M. Fujita, *Chem. Asian J.* **2015**, *10*, 2292–2295; d) D. Fujita, H. Yokoyama, Y. Ueda, S. Sato, M. Fujita, *Angew. Chem. Int. Ed.* **2015**, *54*, 155–158; *Angew. Chem.* **2015**, *127*, 157–160; e) D. Fujita, Y. Ueda, S. Sato, N. Mizuno, T. Kumasaka, M. Fujita, *Nature* **2016**, *540*, 563–566.
- [11] a) K. Suzuki, M. Kawano, M. Fujita, *Angew. Chem. Int. Ed.* **2007**, *46*, 2819–2822; *Angew. Chem.* **2007**, *119*, 2877–2880; b) S. Ganta, D. K. Chand, *Dalton Trans.* **2015**, *44*, 15181–15188; c) W. M. Bloch, Y. Abe, J. J. Holstein, C. M. Wandtke, B. Dittrich, G. H. Clever, *J. Am. Chem. Soc.* **2016**, *138*, 13750–13755; d) C. Klein, C. Gütz, M. Bogner, F. Topić, K. Rissanen, A. Lützen, *Angew. Chem. Int. Ed.* **2014**, *53*, 3739–3742; *Angew. Chem.* **2014**, *126*, 3814–3817; e) D. Samanta, A. Chowdhury, P. S. Mukherjee, *Inorg. Chem.* **2016**, *55*, 1562–1568; f) S. M. Jansze, G. Cecot, M. D. Wise, K. O. Zhurov, T. K. Ronson, A. M. Castilla, A. Finelli, P. Pattison, E. Solari, R. Scopelliti, G. E. Zelinskii, A. V. Vologzhanina, Y. Z. Voloshin, J. R. Nitschke, K. Severin, *J. Am. Chem. Soc.* **2016**, *138*, 2046–2054; g) D. K. Chand, K. Biradha, M. Kawano, S. Sakamoto, K. Yamaguchi, M. Fujita, *Chem. Asian J.* **2006**, *1*, 82–90.
- [12] a) S. Freye, J. Hey, A. Torras-Galán, D. Stalke, R. Herbst-Irmer, M. John, G. H. Clever, *Angew. Chem. Int. Ed.* **2012**, *51*, 2191–2194; *Angew. Chem.* **2012**, *124*, 2233–2237; b) S. Freye, R. Michel, D. Stalke, M. Pawliczek, H. Frauendorf, G. H. Clever, *J. Am. Chem. Soc.* **2013**, *135*, 8476–8479; c) R. Sekiya, M. Fukuda, R. Kuroda, *J. Am. Chem. Soc.* **2012**, *134*, 10987–10997; d) Y.-H. Li, J.-J. Jiang, Y.-Z. Fan, Z.-W. Wei, C.-X. Chen, H.-J. Yu, S.-P. Zheng, D. Fenske, C.-Y. Su, M. Barboiu, *Chem. Commun.* **2016**, *52*, 8745–8748.
- [13] S. Löffler, J. Lübben, L. Krause, D. Stalke, B. Dittrich, G. H. Clever, *J. Am. Chem. Soc.* **2015**, *137*, 1060–1063.
- [14] R. Zhu, J. Lübben, B. Dittrich, G. H. Clever, *Angew. Chem. Int. Ed.* **2015**, *54*, 2796–2800; *Angew. Chem.* **2015**, *127*, 2838–2842.
- [15] a) M. Frank, J. Ahrens, I. Bejenke, M. Krick, D. Schwarzer, G. H. Clever, *J. Am. Chem. Soc.* **2016**, *138*, 8279–8287; b) J. Ahrens, M. Frank, G. H. Clever, D. Schwarzer, *Phys. Chem. Chem. Phys.* **2017**, *19*, 13596–13603.
- [16] W. M. Bloch, J. J. Holstein, W. Hiller, G. H. Clever, *Angew. Chem. Int. Ed.* **2017**, *56*, 8285–8289; *Angew. Chem.* **2017**, *129*, 8399–8404.
- [17] A. Burkhardt, T. Pakendorf, B. Reime, J. Meyer, P. Fischer, N. Stübe, S. Panneerselvam, O. Lorbeer, K. Stachnik, M. Warmer, P. Rödig, D. Göries, A. Meents, *Eur. Phys. J. Plus* **2016**, *131*, 56.
- [18] We use the term “container” to describe the general shape of the Pd<sub>4</sub>L<sub>8</sub> D<sub>4h</sub>-symmetric monomers.
- [19] To obey the D<sub>2d</sub> symmetry of the Pd<sub>8</sub>L<sub>16</sub> catenane, the NO<sub>3</sub><sup>-</sup> anions are expected to rapidly exchange with free NO<sub>3</sub><sup>-</sup> anions in solution.
- [20] We note that catenation of this system is also dependent on CH<sub>3</sub>CN as the solvent. The fact that catenation is not observed in DMSO may be due to DMSO solvent molecules stabilizing or packing more efficiently in the cavity of the D<sub>4h</sub>-symmetric Pd<sub>4</sub>L<sub>8</sub> monomer than CH<sub>3</sub>CN; see Ref. [11a].
- [21] a) D. Li, J. Zhang, K. Landskron, T. Liu, *J. Am. Chem. Soc.* **2008**, *130*, 4226–4227; b) D. Li, W. Zhou, K. Landskron, S. Sato, C. J. Kiely, M. Fujita, T. Liu, *Angew. Chem. Int. Ed.* **2011**, *50*, 5182–5187; *Angew. Chem.* **2011**, *123*, 5288–5293; c) H. Li, J. Luo, T. Liu, *Chem. Eur. J.* **2016**, *22*, 17949–17952; d) Y. Zhang, Q.-F. Zhou, G.-F. Huo, G.-Q. Yin, X.-L. Zhao, B. Jiang, H. Tan, X. Li, H.-B. Yang, *Inorg. Chem.* **2017**, <https://doi.org/10.1021/acs.inorgchem.7b02777>; e) J. K. Clegg et al., *Angew. Chem. Int. Ed.* **2010**, *49*, 1075–1078; *Angew. Chem.* **2010**, *122*, 1093–1096.
- [22] a) D. E. Discher, A. Eisenberg, *Science* **2002**, *297*, 967–973; b) E. F. Marques, O. Regev, A. Khan, B. Lindman, *Adv. Colloid Interface Sci.* **2003**, *100–102*, 83–104; c) M. Sauer, W. Meier, *Chem. Commun.* **2001**, 55–56.
- [23] The broader distribution may be due to partial desolvation and deformation of the vesicle-like aggregates because of solvent loss.
- [24] CCDC 1811308 (**1c**) and 1811309 (**2b**) contain the supplementary crystallographic data for this paper. These data can be obtained free of charge from The Cambridge Crystallographic Data Centre.

Manuscript received: January 12, 2018

Accepted manuscript online: February 1, 2018

Version of record online: March 22, 2018